Geophysical Research Letters

RESEARCH LETTER
10.1029/2023GL106888

Riparian Groundwater Nitrogen (N) Isotopes Reveal Human Imprints of Dams and Road Salt Salinization

Shreeram Inamdar[1], Marc Peipoch[2], Matthew Sena[1], Bisesh Joshi[3], Md. Moklesur Rahman[1], Jinjun Kan[2], Erin K. Peck[1], Arthur Gold[4], Tara L. E. Trammell[1], and Peter M. Groffman[5,6]

[1]Plant & Soil Sciences, University of Delaware, Newark, DE, USA, [2]Stroud Water Research Center, Avondale, PA, USA, [3]Water Science & Policy Graduate Program, University of Delaware, Newark, DE, USA, [4]Department of Natural Resources Science, University of Rhode Island, Kingston, RI, USA, [5]City University of New York Advanced Science Research Center at the Graduate Center, New York, NY, USA, [6]Cary Institute of Ecosystem Studies, Millbrook, NY, USA

Key Points:

- Groundwater N isotopes revealed altered riparian N processing due to milldams and salinization
- Groundwater $\delta^{15}N\text{-}NO_3^-$ values changed along the riparian transect and in response to electron donor to acceptor ($DOC:NO_3^-$) ratios
- Low groundwater $\delta^{15}N\text{-}NO_3^-$ values were attributed to suppression of denitrification due to persistent anoxic conditions and salinization

Supporting Information:

Supporting Information may be found in the online version of this article.

Correspondence to:

S. Inamdar,
inamdar@udel.edu

Citation:

Inamdar, S., Peipoch, M., Sena, M., Joshi, B., Rahman, Md. M., Kan, J., et al. (2024). Riparian groundwater nitrogen (N) isotopes reveal human imprints of dams and road salt salinization. *Geophysical Research Letters*, *51*, e2023GL106888. https://doi.org/10.1029/2023GL106888

Received 18 OCT 2023
Accepted 14 FEB 2024

Abstract Groundwater nitrate-N isotopes ($\delta^{15}N\text{-}NO_3^-$) have been used to infer the effects of natural and anthropogenic change on N cycle processes in the environment. Here we report unexpected changes in groundwater $\delta^{15}N\text{-}NO_3^-$ for riparian zones affected by relict milldams and road salt salinization. Contrary to natural, undammed conditions, groundwater $\delta^{15}N\text{-}NO_3^-$ values declined from the upland edge through the riparian zone and were lowest near the stream. Groundwater $\delta^{15}N\text{-}NO_3^-$ values increased for low electron donor (dissolved organic carbon) to acceptor (NO_3^-) ratios but decreased beyond a change point in ratios. Groundwater $\delta^{15}N\text{-}NO_3^-$ values were particularly low for the riparian milldam site subjected to road-salt salinization. We attributed these N isotopic trends to suppression of denitrification, occurrence of dissimilatory nitrate reduction to ammonium (DNRA), and/or effects of road salt salinization. Groundwater $\delta^{15}N\text{-}NO_3^-$ can provide valuable insights into process mechanisms and can serve as "imprints" of anthropogenic activities and legacies.

Plain Language Summary Human activities and their legacies can alter our environment and the imprints can last for a long time. Here, we show the groundwater stable nitrogen isotopes can provide new and unexpected insights into nitrogen processing and cycling in riparian zones affected by dams and road salt salinization. Using such metrics/indicators we can investigate the changes in process mechanisms and the thresholds at which they change. This knowledge will help us better manage environments impacted by human landuse.

1. Introduction

Human activities and their legacies have significantly altered the amounts, forms, and cycling of nitrogen (N) (Basu et al., 2022; Galloway et al., 2008). Stable isotopes of N have been used successfully to assess some of these anthropogenic changes since they provide an integrated assessment of N processes, sources, and mixing (Burns et al., 2009; Peipoch et al., 2012; Weitzman et al., 2021). Here, we show that changes in groundwater N isotopes can provide important new insights into how damming and salinization can modify the reductive N processes in riparian ecosystems.

The abundance of natural ^{15}N is typically expressed as $\delta^{15}N$ (Bedard-Haughn et al., 2003; Nestler et al., 2011), which represents the isotope ratio (heavier ^{15}N to lighter ^{14}N) of a sample relative to the ratio of a standard (i.e., atmospheric N_2) expressed in parts per mil (‰). The chemical bonds formed by lighter ^{14}N isotopes are weaker and easier to break compared to those with ^{15}N isotopes. This results in isotopic discrimination, or fractionation, leading to increasing amounts of ^{15}N in the substrate (isotopic enrichment) and a higher proportion of the lighter ^{14}N in the product (isotopic depletion) (Kendall et al., 2007). Elevated N concentrations in the substrate can especially favor fractionation and substrate enrichment (Kendall et al., 2007). Similar fractionation also extends to other elements such as oxygen isotopes (e.g., ^{18}O and ^{16}O) that are present in nitrate-N. N cycle processes that enhance fractionation of N isotopes include microbial processes such as nitrification and denitrification, and abiotic processes such a volatilization. Denitrification typically occurs in hydrologically variable, but wet soil conditions, and is strongly fractionating by enriching the $\delta^{15}N$ content of groundwater nitrate-N (as high as 80‰; Bedard-Haughn et al., 2003).

Riparian zones buffer upland N inputs with a progressive decrease in groundwater nitrate-N concentrations from the upland to the stream (Lowrance et al., 1997; Pinay et al., 2018). This N removal has been attributed to denitrification and plant uptake, with denitrification stimulated by increasing supply of soil organic carbon (C) and variable redox conditions closer to the stream (Ranalli & Macalady, 2010; Rivett et al., 2008). Not surprisingly, groundwater nitrate $\delta^{15}N$ ($\delta^{15}N\text{-}NO_3^-$) has been reported to be enriched in the riparian zone (Clement et al., 2003; Sebilo et al., 2003; Vidon & Hill, 2005). Clement et al. (2003) reported a progressive increase in $\delta^{15}N\text{-}NO_3^-$ from +5‰ at the upland edge to +28‰ near the stream for a riparian zone located in a N-rich agricultural watershed in France and attributed it to denitrification. Similar observations were made by Vidon and Hill (2005) for Canadian Shield riparian sites. Alternatively, hydrologic mixing, reduced denitrification and/or other NO_3^- retentive processes could also affect groundwater $\delta^{15}N\text{-}NO_3^-$ enrichment and need to be accounted for (Dhondt et al., 2003; Lutz et al., 2020; Wang et al., 2023).

Riparian N processing can be altered by anthropogenic influences such as dams and/or salinization (Herbert et al., 2015; Inamdar et al., 2022; Lewis et al., 2021) with potential cascading effects for riparian groundwater $\delta^{15}N\text{-}NO_3^-$. Milldams dampen the variability of stream water levels upstream of the dam resulting in stagnant, near-surface groundwater levels, and persistent hypoxia/anoxia in near-stream riparian soils (Sherman et al., 2022). Persistent anoxic soils that increase electron donor (e.g., organic C and iron (Fe)) to acceptor (NO_3^-) ratio in soils have been found to favor obligate anaerobes such as those associated with dissimilatory nitrate reduction to ammonium (DNRA; a process that retains N in soils) versus the facultative microorganisms that drive N removal via denitrification (Burgin & Hamilton, 2007; Giblin et al., 2013; Tiedje, 1988). Under high organic C to nitrate-N ratios, DNRA has advantage over denitrification since more electrons (eight vs. five) can be transferred per mole of nitrate-N yielding higher energy for DNRA (Tiedje, 1988). But, how DNRA alters $\delta^{15}N\text{-}NO_3^-$ is unknown (Denk et al., 2017; Nikolenko et al., 2018). Similarly, salinization of soils suppresses denitrification rates through direct and indirect effects on electron transfer and reductive enzymes while simultaneously enhancing N mineralization and DNRA (Herbert et al., 2015); which could further affect groundwater $\delta^{15}N\text{-}NO_3^-$.

Our recent work on two riparian sites upstream of 200+ year old milldams revealed riparian groundwater N concentrations and processing unlike that reported for dynamic, natural, riparian systems (Inamdar et al., 2022; Peck et al., 2022). While groundwater nitrate-N concentrations declined through the riparian transect (upland to the stream), ammonium-N concentrations were highest in the persistently hypoxic/anoxic groundwaters upstream of the milldam and adjacent to the stream (Inamdar et al., 2022). The high groundwater ammonium concentrations were attributed to anaerobic N mineralization, suppression of nitrification, and/or DNRA. Potential denitrification rates were highest at the upland riparian edge and lowest at the persistently saturated near-stream position (Peck et al., 2022). Furthermore, soil denitrification rates and denitrification functional genes (*nosZ*) were lower for the road-salt affected riparian soils suggesting potential suppression of denitrification by salinization (Kan et al., 2023; Peck et al., 2022).

Given the complex and coupled effects of milldams and salinization on riparian N cycle processes, we explored whether $\delta^{15}N\text{-}NO_3^-$ signatures could characterize these effects and provide additional insights into the key processes and specific drivers involved. We hypothesized that changes in N processing due to dams and salinization would cascade and alter the riparian groundwater $\delta^{15}N\text{-}NO_3^-$ signatures. We propose that while natural riparian conditions would typically result in a progressive denitrification-driven enrichment of groundwater $\delta^{15}N\text{-}NO_3^-$ through the riparian zone (Figure 1a), the same $\delta^{15}N\text{-}NO_3^-$ regime will not be observed for riparian groundwaters upstream of milldams and affected by salinization (Figure 1b). While some $\delta^{15}N\text{-}NO_3^-$ enrichment may be observed at the more hydrologically dynamic and nitrate-rich upland-edge (Figure 1b), the near-stream soils with persistently hypoxic conditions, high electron donor (OC and reduced Fe) to acceptor (NO_3^-) ratio, nitrate-poor conditions, and low denitrification (Peck et al., 2022), would result in depleted groundwater $\delta^{15}N\text{-}NO_3^-$ values (Figure 1b). We further predict a change in riparian groundwater $\delta^{15}N\text{-}NO_3^-$ when the denitrification-driven enrichment regime at low donor to acceptor ratio and high NO_3^- concentrations shifts to a high donor:acceptor and low NO_3^- DNRA regime (Figure 1c). Finally, suppression of denitrification by salinization could further lower the groundwater $\delta^{15}N\text{-}NO_3^-$ (Figure 1c). We test these hypotheses using stream water and groundwater $\delta^{15}N\text{-}NO_3^-$ and $\delta^{18}O\text{-}NO_3^-$ data collected over 3 years (2020–2022) for the two milldam-affected riparian sites. To our knowledge, this is the first study investigating how riparian groundwater $\delta^{15}N\text{-}NO_3^-$ can be affected by milldams and salinization and subsequent alteration in electron donor:acceptor ratios. If groundwater $\delta^{15}N\text{-}NO_3^-$ values are sensitive to anthropogenic alteration of N processing, they could serve as a valuable "fingerprints" or tools to assess these impacts at the landscape scale, as well as, discriminate between individual N processes.

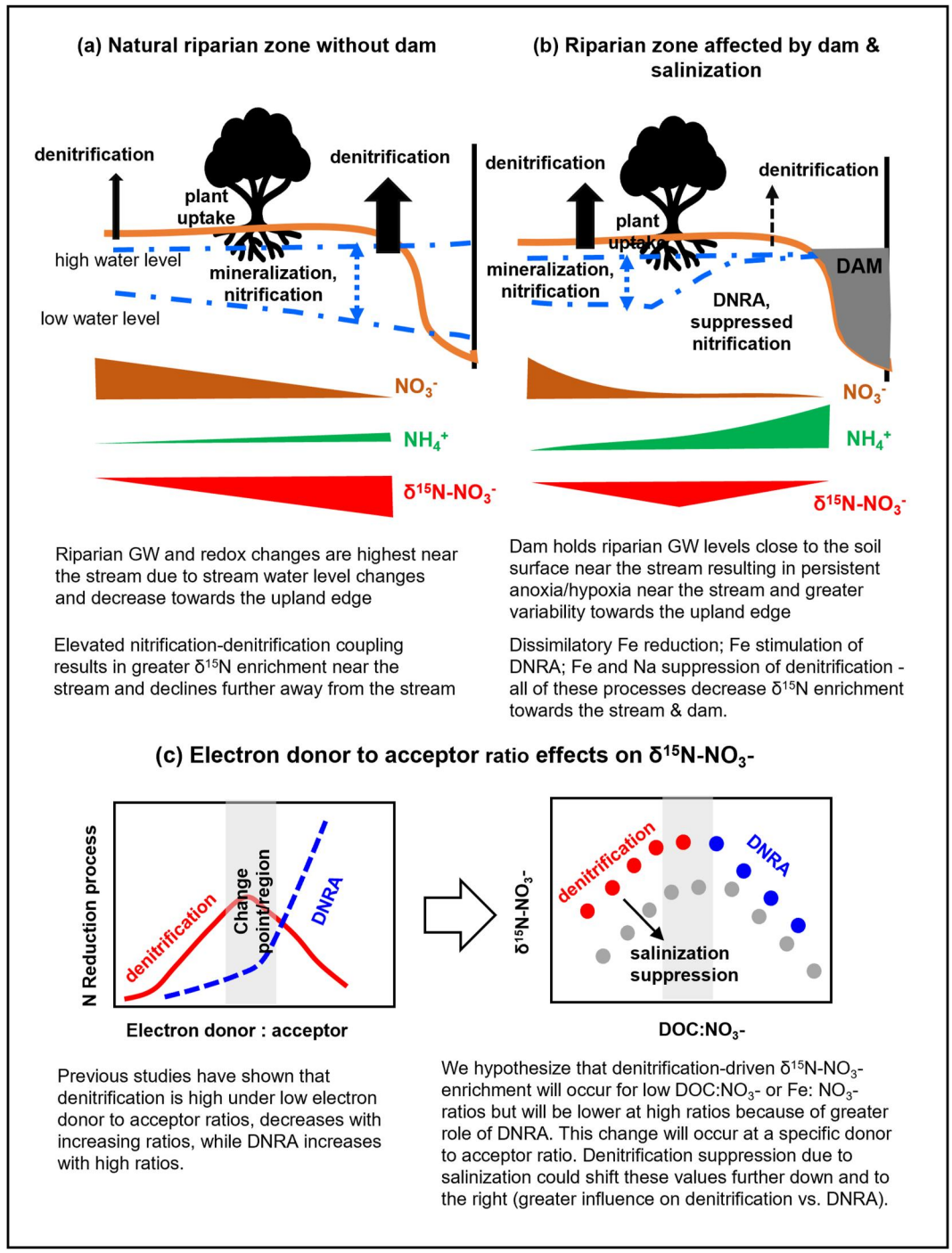

Figure 1. Conceptual model characterizing the changes in groundwater $\delta^{15}N\text{-}NO_3$: (a) along the riparian transect for natural ecosystems; (b) for riparian zones affected by dams and road salt salinization; and (c) for varying electron donor (DOC) to acceptor (NO_3^-) ratios.

2. Materials and Methods

Detailed descriptions of the riparian study sites and sampling procedures were previously reported in Inamdar et al. (2022), Sherman et al. (2022), and Peck et al. (2022). Riparian zones upstream of the Roller milldam (2.4 m tall; coordinates 40.108306, −76.443111) on Chiques Creek in Pennsylvania and the Cooch milldam (4 m tall; coordinates 39.645556, −75.742500) on Christina River in Delaware were studied (Figure S1 in Supporting

Information S1). The drainage area in the Chiques Creek watershed (127 km^2 at dam) is primarily agricultural while mixed landuse dominates in the Christina River watershed (50.7 km^2). The riparian zone at the Cooch site is also immediately downstream of a major interstate highway (I-95) which receives substantial winter deicing road salt applications. Mean annual air temperature is 15.5 and 12.2°C for Roller and Cooch sites, respectively, while mean annual precipitation is 104 and 114 cm (NOAA, 2021). The sediments upstream of the dam at both riparian sites were predominantly silt and clay (56%–100%; Peck et al., 2022) with thickness of the riparian sediments varying between 1 and 4 m depending on the height of the dam. Organic matter in the upstream riparian sediments varied between 0.7% and 9.8% (Peck et al., 2023). Sodium (Na^+) at the road-salt affected Cooch site was significantly greater than Roller for both soil (mean 293 vs. 38 mg kg^{-1}, respectively) and groundwater (mean 199 vs. 33 mg L^{-1}, respectively) (Inamdar et al., 2022).

The geology of the Chiques Creek watershed is composed predominantly of dolomite/limestone (40%) and shale (30%) (DCNR, 2021). The Cooch's Mill area is in the Piedmont physiographic province with the primary geologic unit being Iron Hill gabbro, a deeply weathered rock rich in iron oxides (Ramsey, 2005). Instrumented riparian areas at both milldam sites were forested and included sugar maple (*Acer saccharum*), black walnut (*Juglans nigra*), and American sycamore (*Platanus occidentalis*) among other species.

Three groundwater well transects (T1-T3) with three wells each (W1-W3) were established upstream of the Roller dam, whereas at Cooch, two well transects (T1 and T2) with two wells (W1 and W2) each were installed upstream of the dam (Sherman et al., 2022) (Figure S1 in Supporting Information S1). These wells were instrumented with Hobo water level loggers (U20L) that recorded groundwater elevations and temperature every 30 min. High frequency (30 min) dissolved oxygen (DO) sensors (Hobo U26) were also installed in select wells (at Roller T1W1 and T1W3) to characterize groundwater DO. Manual grab water sampling for stream water and groundwater has been conducted monthly since November 2019 with all sampling occurring during non-storm conditions. All water samples were filtered using a glass microfiber filter (0.7 μm) and analyzed for dissolved organic carbon (DOC) on an Elementar Vario-Cube TOC Analyzer; ammonium-N and nitrate-N colorimetrically using a Bran&Luebbe AutoAnalyzer 3; and total dissolved Fe (TdFe) and Na^+ by inductively coupled plasma optical emission spectroscopy using an iCAP 7600 Duo View ICP-OES (Inamdar et al., 2022).

Selected monthly stream and groundwater subsamples were analyzed for $\delta^{15}N\text{-}NO_3^-$ and $\delta^{18}O\text{-}NO_3^-$. Cooch samples were analyzed for: September and November, 2020; April and November, 2021; and May–June, August–October, 2022; while at Roller the sampled dates were: September and November, 2020; March, April, July, and October, 2021; and May–September 2022. Because of varying lab openings over the Covid-19 pandemic period, the isotopes were analyzed at three separate full-service labs: 2020 samples were analyzed at the University of Pittsburg Isotope Laboratory by the denitrifier method (Casciotti et al., 2002); 2021 samples at the University of Waterloo Isotope Laboratory by the denitrifier method; and the 2022 samples at the University of Nebraska Water Center using the titanium trichloride method.

All statistical analysis was performed using JMP and R software. Significant differences were determined using paired *t* tests ($\alpha = 0.05$) while regression analysis was performed using Pearson and piece-wise (Muggeo, 2008) regression. Data from all wells and stream locations were used to assess the isotopic differences between the two riparian sites. To evaluate the changes in groundwater $\delta^{15}N\text{-}NO_3^-$ and $\delta^{18}O\text{-}NO_3^-$ along the riparian transect, data from only transect 1 (T1) at the Roller riparian site were used since this site had three wells along the transect (as opposed to Cooch that had only two wells), the groundwater flow direction was orthogonal to the stream, revealed the largest changes in groundwater nitrate-N (Inamdar et al., 2022; Sherman et al., 2022), and this transect was assessed for changes in soil denitrification rates (Peck et al., 2022).

3. Results

3.1. Distinct Differences Between the Salt-Affected Cooch Versus the Roller Riparian Sites

Riparian groundwater $\delta^{15}N\text{-}NO_3^-$ values for Cooch were lower (−9.62–4.82‰; mean −0.79‰) and significantly different from Roller groundwater (−9.9–29.96‰; mean 9.07‰) and Cooch stream water (Figure 2 and Table S1 in Supporting Information S1). In contrast, the stream water $\delta^{15}N\text{-}NO_3^-$ values for the two watersheds were not significantly different. Most of the Cooch groundwater $\delta^{15}N\text{-}NO_3^-$ values fell within the ranges of soil and NH_4^+ in rain (Figure 2). On the other hand, Roller groundwater values were higher (shifted to the right) and a few fell within the slope region ($\delta^{18}O\text{-}NO_3^-$:$\delta^{15}N\text{-}NO_3^-$ = 1:1–1:2) designated for denitrification.

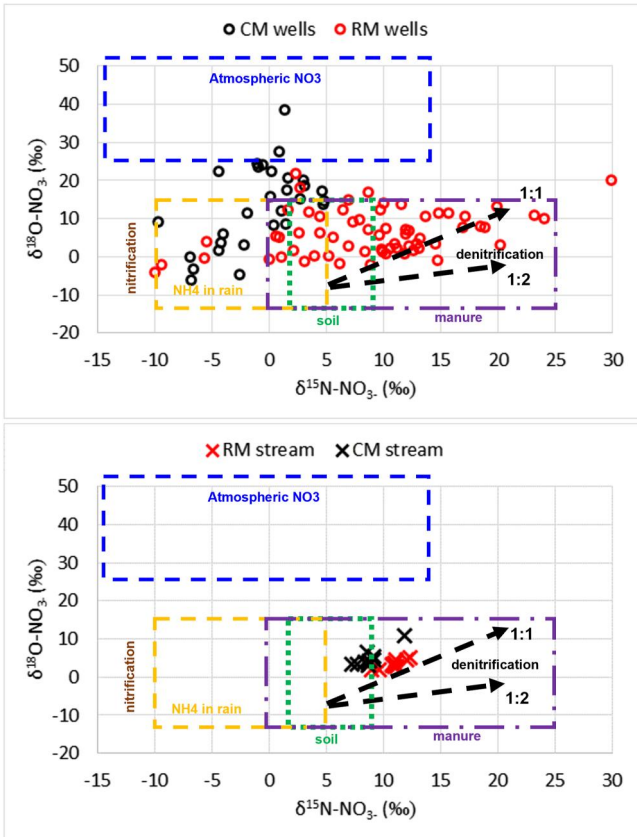

Figure 2. $\delta^{15}N\text{-}NO_3^-$ versus $\delta^{18}O\text{-}NO_3^-$ for groundwaters (top panel) and stream water (bottom panel) for Cooch (CM, black) and Roller (RM, red) sites. Isotopic bounds for various N sources and processes (nitrification and denitrification) reported by Kendall et al. (2007) are also included. Denitrification is indicated within the slope region ($\delta^{18}O\text{-}NO_3^-$: $\delta^{15}N\text{-}NO_3^-$ = 1:1–1:2).

Similar to $\delta^{15}N\text{-}NO_3^-$, riparian groundwater $\delta^{18}O\text{-}NO_3^-$ for Cooch (mean 13.07‰) was significantly different from Roller groundwater (5.98‰) and Cooch stream water values (Table S1 in Supporting Information S1). The streamwater $\delta^{18}O\text{-}NO_3^-$ values for the two watersheds were not different (Table S1 in Supporting Information S1). While most of the Cooch $\delta^{18}O\text{-}NO_3^-$ values fell within the nitrification region, a couple of the values were in the atmospheric NO_3^- range (Figure 2).

Nitrate-N concentrations were highest for Roller groundwater at the upland-edge well (T1W3) with other Roller and Cooch groundwaters having very low nitrate-N concentrations (Figures 3a and 4b). Low groundwater $\delta^{15}N\text{-}NO_3^-$ values, especially those for Cooch, corresponded with elevated ammonium N concentrations (Figure 3b) which were significantly greater for Cooch versus Roller (Table S1 in Supporting Information S1). However, the most pronounced differences between Cooch versus Roller groundwaters were with regard to Na^+ and TdFe concentrations—both significantly elevated at Cooch (Figures 3c and 3d and Table S1 in Supporting Information S1). Our laboratory assessments using Ferrozine aasays (data not included) confirmed that most of the TdFe was in Fe^{2+} form.

A comparison of groundwater $\delta^{15}N\text{-}NO_3^-$ values versus $DOC\text{:}NO_3^-$ (electron donor to acceptor ratio) (Figure 3e) revealed a potential change in groundwater $\delta^{15}N\text{-}NO_3^-$ around a ratio of 0.55–2. Below a ratio of 2.09, groundwater $\delta^{15}N\text{-}NO_3^-$ displayed an increasing trend, while >2.09 the trend was decreasing. A piece-wise regression analysis selected a $DOC\text{:}NO_3^-$ ratio of 0.55 as the change point (Figure S2 in Supporting Information S1, indicated by the vertical dashed line), with opposing linear trends before and after the change point. There was, however, considerable error associated with this change point (indicated by shaded region and error estimate in Figure S2 of the Supporting Information S1) and the error bounds extended to the $DOC\text{:}NO_3^-$ ratio of 2.09. The error range was likely because of absence of additional data points between $DOC\text{:}NO_3^-$ ratios of 0.55 and 2.09. Furthermore, groundwater $\delta^{15}N\text{-}NO_3^-$ values for the salt-affected Cooch site were shifted to the extreme right with high $DOC\text{:}NO_3^-$ ratios of 33–6,600 but lower $\delta^{15}N\text{-}NO_3^-$ values in comparison to Roller (Figure 3e).

3.2. Changes in Groundwater $\delta^{15}N\text{-}NO_3^-$ Along the Roller Riparian Transect (Upland to Stream)

Distinct shifts in groundwater $\delta^{15}N\text{-}NO_3^-$ values and their relationships with solutes from the upland to the stream edge at the Roller riparian transect T1 underscored important differences in N processing (Figure 4). There was a significant linear relationship (R^2 = 0.62; p = 0.004; n = 11) between groundwater $\delta^{15}N\text{-}NO_3^-$ and $\delta^{18}O\text{-}NO_3^-$ values for the upland edge well (RMT1W3) with a slope 0.65 (Figure 4a). This same well displayed an inverse pattern (R^2 = 0.18; p = 0.18; n = 11) between nitrate-N concentrations and $\delta^{15}N\text{-}NO_3^-$ values (Figure 4b). The inverse pattern for nitrate-N was not because of groundwater mixing or dilution since the same relationship was observed when the nitrate-N was normalized by magnesium (Figure S3 in Supporting Information S1); a solute that was previously used as a conservative tracer by Sherman et al. (2022). In comparison, the relationships between $\delta^{15}N\text{-}NO_3^-$ and $\delta^{18}O\text{-}NO_3^-$ and $\delta^{15}N\text{-}NO_3^-$ and nitrate-N did not extend for groundwater at wells RMT1W2 and RMT1W1 located closer to the stream (Figures 4a and 4b). Groundwaters at RMT1W3 also displayed a strong relationship between groundwater temperature and $\delta^{15}N\text{-}NO_3^-$ values (R^2 = 0.50; p = 0.01; n = 11; Figure 4c); which did not extend to the other riparian wells along the transect. The low values of groundwater $\delta^{15}N\text{-}NO_3^-$ for the well closest to the stream (RMT1W1) were however inversely related to elevated ammonium concentrations (Figure 4d).

When groundwater $\delta^{15}N\text{-}NO_3^-$ versus $DOC\text{:}NO_3^-$ ratio were compared for the Roller ransect (Figure 4e), the upland-edge well (RMT1W3) with elevated $\delta^{15}N\text{-}NO_3^-$ had $DOC\text{:}NO_3^-$ ratios less than 2. In contrast, except for

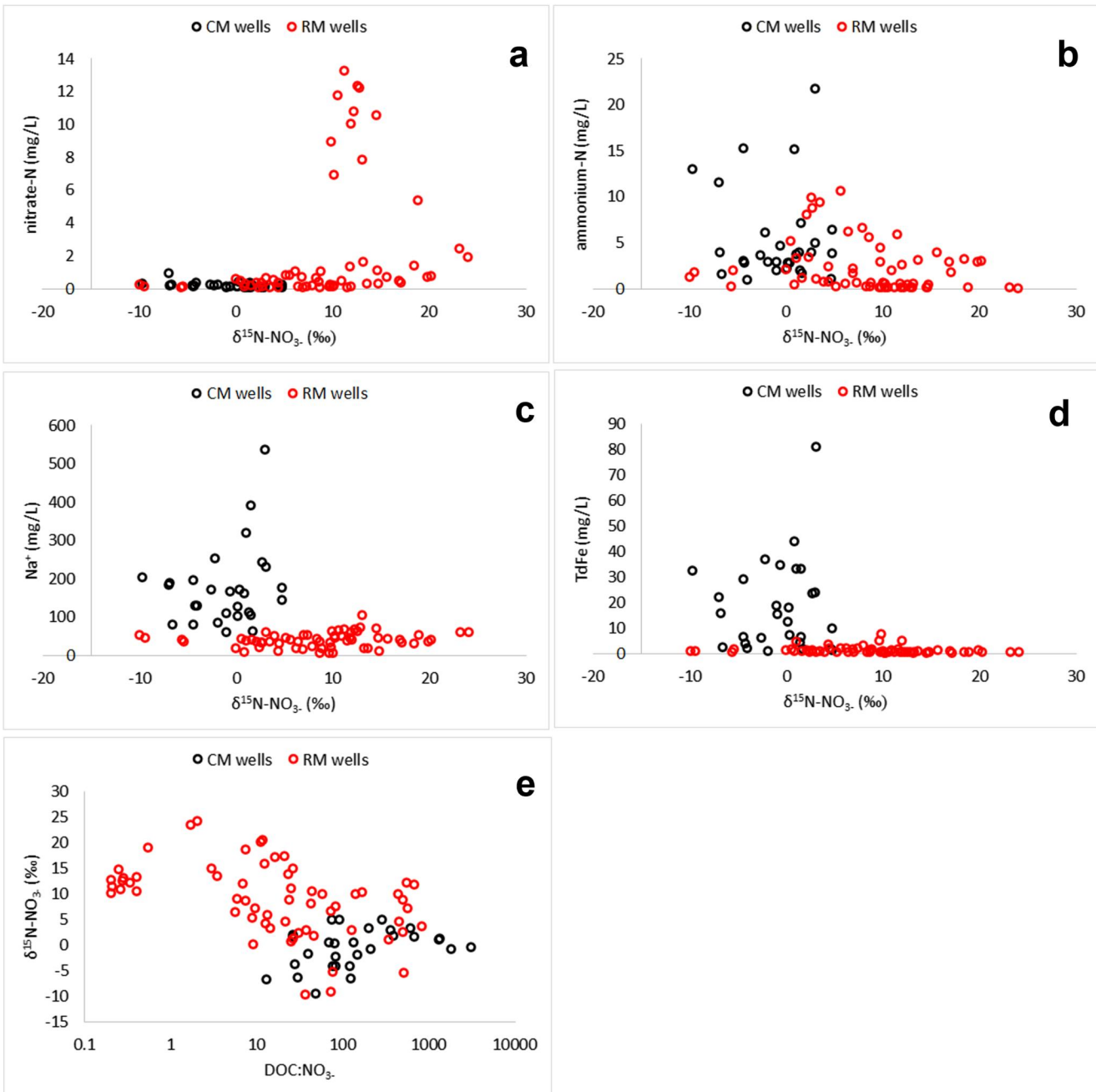

Figure 3. Comparison of Cooch (CM) and Roller (RM) riparian groundwaters and stream water for (a) nitrate-N versus $\delta^{15}N\text{-}NO_3^-$; (b) ammonium-N versus $\delta^{15}N\text{-}NO_3^-$; (c) sodium ($Na^+$) versus $\delta^{15}N\text{-}NO_3^-$; (d) total dissolved Fe (TdFe) versus $\delta^{15}N\text{-}NO_3^-$; and (e) electron donor to acceptor ratio ($DOC:NO_3^-$) versus $\delta^{15}N\text{-}NO_3^-$.

a few values associated with well RMT1W2 and RMT1W1, all other groundwater $\delta^{15}N\text{-}NO_3^-$ values with a $DOC:NO_3^-$ ratio >2 were depleted (or less enriched).

4. Discussion

This study revealed distinct patterns of riparian groundwater $\delta^{15}N\text{-}NO_3^-$ that: (a) were contrary to those typically reported for natural, dynamic riparian systems (Figure 1a); and (b) varied systematically with electron donor to acceptor ($DOC:NO_3^-$) ratios. We attribute this isotopic response to the cascading effects of N processing

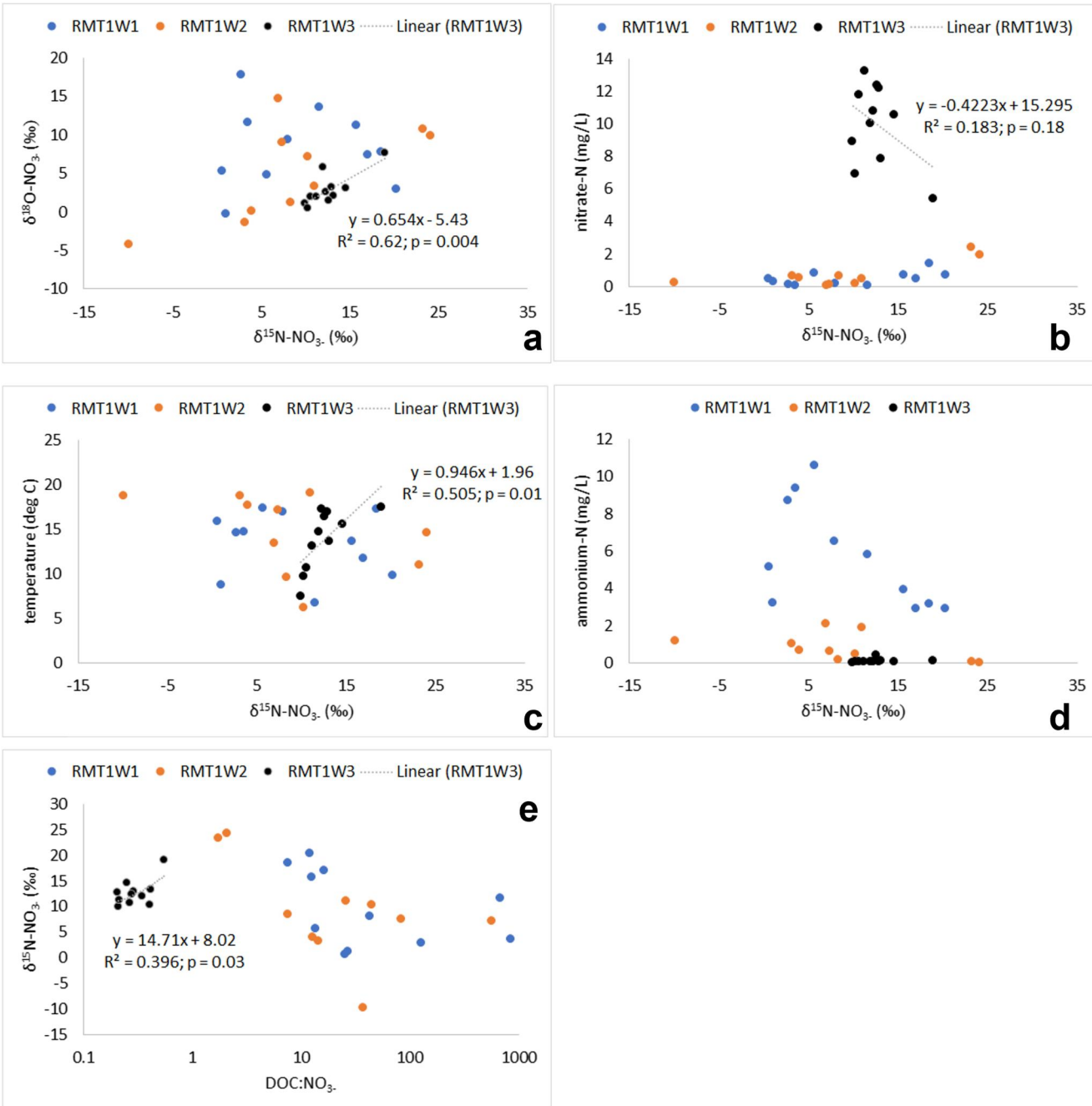

Figure 4. Bivariate plots of Roller transect 1 groundwater values for (a) $\delta^{15}N\text{-}NO_3^-$ versus $\delta^{18}O\text{-}NO_3^-$; (b) nitrate-N versus $\delta^{15}N\text{-}NO_3^-$; (c) groundwater temperatures versus $\delta^{15}N\text{-}NO_3^-$; (d) ammonium-N versus $\delta^{15}N\text{-}NO_3^-$; (e) electron donor to acceptor ratio ($DOC:NO_3^-$) versus $\delta^{15}N\text{-}NO_3^-$.

influenced by milldams and road-salt salinization. We elaborate on these observations and discuss the key responsible mechanisms.

4.1. Milldam Hydrology and N Processing Regulates Groundwater $\delta^{15}N\text{-}NO_3^-$ Along the Riparian Transect

Groundwater $\delta^{15}N\text{-}NO_3^-$ values for Roller were highest at the upland riparian edge (well T1W3) and declined rapidly through the riparian zone with lower values for groundwaters closer to the stream (well T1W1). The slope of the relationship between groundwater $\delta^{15}N\text{-}NO_3^-$ and $\delta^{18}O\text{-}NO_3^-$ of 0.65 (Figure 4a), inverse relationship

between $\delta^{15}N\text{-}NO_3^-$ and NO_3^- (Figure 4b) and the strong correlation between $\delta^{15}N\text{-}NO_3^-$ and temperature (Figure 4c) taken together, suggests that denitrification was the key mechanism responsible for $\delta^{15}N\text{-}NO_3^-$ enrichment at the upland riparian edge, with a lack of a similar response for near-stream groundwaters. Slopes of $\delta^{15}N\text{-}NO_3^-$ versus $\delta^{18}O\text{-}NO_3^-$ between 0.5 and 1 are attributed to denitrification enrichment (Burns et al., 2009; Nikolenko et al., 2018), while the inverse relationship between nitrate-N and $\delta^{15}N\text{-}NO_3^-$ indicates denitrification consumption of nitrate-N with simultaneous enrichment of $\delta^{15}N\text{-}NO_3^-$ (Kendall et al., 2007). Similarly, the positive correlation of $\delta^{15}N\text{-}NO_3^-$ with temperature may be an expression of microbially driven process like denitrification (Matiatos et al., 2021).

The riparian transect pattern of groundwater $\delta^{15}N\text{-}NO_3^-$ observed here is contrary to that of Clement et al. (2003) and Vidon and Hill (2005) who reported progressively increasing groundwater $\delta^{15}N\text{-}NO_3^-$ enrichment from the upland to the stream with highest values closest to the stream. Both studies were for natural riparian zones (without dam) and in agricultural watersheds with elevated groundwater nitrate concentrations. While one of our riparian sites was also in an agricultural watershed (Chiques Creek) with elevated stream (3.4–5.9 mgN L^{-1}) and groundwater (RMT1W3: 5.5–13.2 mg L^{-1}) nitrate-N concentrations, the riparian hydrology and biogeochemical conditions for the Roller site were strongly influenced by the milldam.

Previous hydrologic characterization of the Roller riparian site by Sherman et al. (2022) indicated that while the groundwater variability was high at the upland riparian edge (RMT1W3), near-stream groundwaters were less variable and poorly mixed. This disparity also extended to groundwater DO levels with persistently hypoxic/anoxic conditions near-stream (well RMT1W1) but greater variability at the upland edge (RMT1W3) (Figure 2b in Inamdar et al., 2022 and Figure S4 in Supporting Information S1 here for high frequency sensor DO data).

Dynamic groundwater and redox variations are favored to stimulate coupled nitrification-denitrification processes and facultative denitrification microbes (Peralta et al., 2013; Shi et al., 2020; Tomasek et al., 2019; Ye et al., 2017) that enhance enrichment of $\delta^{15}N\text{-}NO_3^-$. We believe these conditions were responsible for the $\delta^{15}N\text{-}NO_3^-$ enriched groundwater at the upland edge at Roller (well RMT1W3). Indeed, previously measured soil denitrification potentials at the Roller site were highest for the upland edge and declined closer to the stream (Figure 4 in Peck et al., 2022). In contrast to the dynamic conditions that favor denitrification, stagnant hydrologic conditions, persistent soil saturation and anoxia (e.g., well RMT1W1 in Figure S4 of the Supporting Information S1) promote obligate anaerobes and processes like DNRA that compete with denitrification (Chen et al., 2021; Jäntti et al., 2021; Palacin-Lizarbe et al., 2019; Reverey et al., 2018) and could have influenced the $\delta^{15}N\text{-}NO_3^-$ values. Alternatively, it is also highly likely that decreasing groundwater NO_3^- concentrations through the riparian zone may have suppressed the denitrification enrichment of $\delta^{15}N\text{-}NO_3^-$ for near-stream groundwaters.

Previous studies have attributed changes/depletion in $\delta^{15}N\text{-}NO_3^-$ to multiple factors including hydrologic mixing (Lutz et al., 2020) and nitrification (Roberts et al., 2023). Our data (Figure S3 in Supporting Information S1) did not suggest mixing-related effects, and near-stream groundwaters were too hypoxic/anoxic and ammonium-N concentrations too high to suggest nitrification driven $\delta^{15}N\text{-}NO_3^-$ depletion. Dhondt et al. (2003) found low enrichment of groundwater $\delta^{15}N\text{-}NO_3^-$ during winter time for a riparian zone in France and attributed it to DNRA or microbial immobilization. Not surprisingly, both Lutz et al. (2020) and Dhondt et al. (2003) called for greater attention to processes like DNRA, annamox, and microbial assimilation in influencing riparian groundwater $\delta^{15}N\text{-}NO_3^-$ values.

Reducing sediment conditions can also result in the reductive dissolution of iron oxides and concomitant release of Fe^{2+} and DOC (Pan et al., 2016). While low concentrations of Fe^{2+} can stimulate denitrification (Straub et al., 1996), elevated Fe^{2+} concentrations can have a toxic effect for bacterial cells (Carlson et al., 2012; Wang et al., 2020) leading to suppression of denitrification (Rahman et al., 2019; Robertson et al., 2016). Thus, when Fe^{2+} availability is high (as observed for the Cooch site), chemolithotrophic DNRA organisms may have particular metabolic advantages over denitrifying organisms (Pandey et al., 2020; Robertson & Thamdrup, 2017). How DNRA directly affects groundwater $\delta^{15}N\text{-}NO_3^-$ is unknown (Denk et al., 2017; Nikolenko et al., 2018), but given the low nitrate-N concentrations under which it typically occurs, an enrichment effect is likely not possible.

Elevated Fe^{2+} concentrations (and specific mineral forms) could also stimulate abiotic N reduction processes (Hansen et al., 1996). These Fe-driven abiotic processes could yield depleted $\delta^{15}N\text{-}NO_3^-$ values because the reactions occur outside the cell membrane (Chen et al., 2020; Wang et al., 2023). This could also be a possibility

for the Cooch soils where amorphous iron oxides likely contributed to the high TdFe concentrations in groundwaters (Inamdar et al., 2022). Whether such Fe minerals exist at the Cooch site and contribute to abiotic N isotopic changes needs to be investigated. Thus, any or all of these mechanisms could likely be responsible for the low groundwater $\delta^{15}N\text{-}NO_3^-$ values we observed for the near-stream groundwaters and the shift of groundwater $\delta^{15}N\text{-}NO_3^-$ values with DOC:NO_3^- ratios (Figure 4e).

Controlled laboratory experiments investigating the specific controls of DOC to NO_3^- ratios on denitrification-DNRA partitioning have indicated that high (>10–15) ratios favor DNRA (Chen et al., 2022; Rutting et al., 2011). Similarly, using a modeling study, Zhu et al. (2023) reported that denitrification contributes to 100% of NO_3^- reduction at a C:N ratio of 3 but decreases thereafter with DNRA contributing to 80% of NO_3^- reduction at C:N ratio of 10. Here, we used field-based groundwater $\delta^{15}N\text{-}NO_3^-$ values as proxies for potential denitrification-DNRA process rates (Figure 3e and Figure S2 in Supporting Information S1) which were collected over multiple seasons and years and likely included the effects of other electron donors (e.g., Fe^{2+}). It is not surprising then that our data yielded a change in $\delta^{15}N\text{-}NO_3^-$ values (Figure S2 in Supporting Information S1) at lower DOC to NO_3^- ratios. The patterns of $\delta^{15}N\text{-}NO_3^-$, however, suggest that these values could serve as a valuable proxy for characterizing denitrification-DNRA partitioning in riparian groundwaters and that these results support the hypothesis presented in Figure 1c. We recognize though that there was considerable error associated with the change point/region (DOC to NO_3^- ratios >0.55 and <3) in Figure S2 of the Supporting Information S1 and that additional groundwater data (including more riparian well transects and sites) should be collected for rigorous confirmation of this change point. The ratio could also be affected by the lability or quality of DOC. Future studies should also explicitly determine the rates of denitrification and DNRA and their relationships with groundwater $\delta^{15}N\text{-}NO_3^-$ values. Indeed, our ongoing research at these sites has recently confirmed the occurrence of DNRA, and how it alters groundwater $\delta^{15}N\text{-}NO_3^-$ is values is planned.

4.2. Road-Salt Salinization and Groundwater $\delta^{15}N\text{-}NO_3^-$ Depletion

Groundwater $\delta^{15}N\text{-}NO_3^-$ values for the salt-affected Cooch site were significantly lower compared to the Roller riparian site (Figure 3c). We attribute these depleted groundwater $\delta^{15}N\text{-}NO_3^-$ values to suppressed denitrification and potentially higher DNRA and anaerobic mineralization in riparian soils at the Cooch site. Indeed, our previous measurements of denitrification potentials (Peck et al., 2022) as well as *nosZ* denitrification genes (Kan et al., 2023), indicated lower values for the Cooch versus the Roller site. We believe that the suppressed denitrification and higher DNRA at Cooch were a coupled result of milldam induced reducing conditions and presence of naturally occurring iron-rich soils amplified by effects of Na^+ from road-salt salinization (Inamdar et al., 2022).

Sodium can have a dispersive effect on clay-rich sediments and impede the diffusion of oxygen leading to more anoxic conditions that favor DNRA (Herbert et al., 2015). Sodium can also displace Fe^{2+} off sorption surfaces (Baldwin et al., 2006) and increase the reduction of iron oxides, resulting in increased availability of Fe^{2+} for DNRA (Weston et al., 2010) and/or iron-driven abiotic N processes (Wang et al., 2023; Weber et al., 2006). Salinization has also been found to have a direct suppressive effect on denitrification microbes (Morina & Franklin, 2022; Neubauer et al., 2019). All of these factors and their cascading N effects likely contributed to the more depleted groundwater $\delta^{15}N\text{-}NO_3^-$ values recorded at Cooch supporting the hypothesis presented in Figure 1c.

5. Conclusions

This study revealed novel insights into how altered biogeochemical environment and N processing due to milldams and road-salt salinization can cascade to modify the natural N isotopic regime of riparian groundwaters. Key results were: (a) persistent reducing conditions upstream of milldams suppressed the enrichment of groundwater $\delta^{15}N\text{-}NO_3^-$ near the stream; (b) ground water $\delta^{15}N\text{-}NO_3^-$ displayed a change in values against electron donor to acceptor (DOC:NO_3^-) ratios with enrichment at ratios <2 and depletion of $\delta^{15}N\text{-}NO_3^-$ values for ratios >2; (c) further depletion of groundwater $\delta^{15}N\text{-}NO_3^-$ values was observed for a riparian site impacted by road-salt salinization (high Na^+ concentrations). We attributed the depleted $\delta^{15}N\text{-}NO_3^-$ isotopic composition to suppression of denitrification and/or occurrence of DNRA, but additional work is needed to explicitly test this linkage.

Understanding of how N isotopic signatures change as a result of human alterations of N reductive processes is valuable and will allow for their use as important water quality indicators or finerprints of athropogenic activity.

For example, groundwater N isotopes could be leveraged to assess if riparian buffers are effective for permanent N removal—absence of sustained denitrification N enrichment would discount this possibility. Similarly, in conjunction with process measurements, $\delta^{15}N\text{-}NO_3^-$ values could also be used in laboratory and field experiments to discriminate between denitrification and DNRA and/or other N processes.

Data Availability Statement

All water and isotope chemistry data used in this manuscript is publicly available at Inamdar et al. (2024).

Acknowledgments
We thank the Koser and the Cooch families for permissions to work on their property. This study was funded by National Science Foundation Hydrologic Sciences Grants 1929747 and 2213855.

References

Baldwin, D., Rees, G. N., Mitchell, A. M., Watson, G., & Williams, J. (2006). The short-term effects of salinization on anaerobic nutrient cycling and microbial community structure in sediment from a freshwater wetland. *Wetlands*, *26*(2), 455–464. https://doi.org/10.1672/0277-5212(2006)26[455:tseoso]2.0.co;2

Basu, N. B., Van Meter, K. J., Byrnes, D. K., Van Cappellen, P., Brouwer, R., Jacobsen, B. H., et al. (2022). Managing nitrogen legacies to accelerate water quality improvement. *Nature Geoscience*, *15*(2), 97–105. https://doi.org/10.1038/s41561-021-00889-9

Bedard-Haughn, A., Van Groenigen, J. W., & Van Kessel, C. (2003). Tracing ^{15}N through landscapes: Potential uses and precautions. *Journal of Hydrology*, *272*(1–4), 175–190. https://doi.org/10.1016/s0022-1694(02)00263-9

Burgin, A. J., & Hamilton, S. K. (2007). Have we overemphasized the role of denitrification in aquatic ecosystems? A review of nitrate removal pathways. *Frontiers in Ecology and the Environment*, *5*(2), 89–96. https://doi.org/10.1890/1540-9295(2007)5[89:hwotro]2.0.co;2

Burns, D. A., Boyer, E. W., Elliott, E. M., & Kendall, C. (2009). Sources and transformations of nitrate from streams draining varying land uses: Evidence from dual isotope analysis. *Journal of Environmental Quality*, *38*(3), 1149–1159. https://doi.org/10.2134/jeq2008.0371

Carlson, H. K., Clark, I. C., Melnyk, R. A., & Coates, J. D. (2012). Toward a mechanistic understanding of anaerobic nitrate-dependent iron oxidation: Balancing electron uptake and detoxification. *Frontiers in Microbiology*, *3*. https://doi.org/10.3389/fmicb.2012.00057

Casciotti, K. L., Sigman, D. M., Hastings, M. G., Böhlke, J. K., & Hilkert, A. (2002). Measurement of the oxygen isotopic composition of nitrate in seawater and freshwater using the denitrifier method. *Analytical Chemistry*, *74*(19), 4905–4912. https://doi.org/10.1021/ac020113w

Chen, G., Chen, D., Li, F., Liu, T., Zhao, Z., & Cao, F. (2020). Dual nitrogen-oxygen isotopic analysis and kinetic model for enzymatic nitrate reduction coupled with Fe (II) oxidation by Pseudogulbenkiania sp. strain 2002. *Chemical Geology*, *534*, 119456. https://doi.org/10.1016/j.chemgeo.2019.119456

Chen, Y., Leung, P. M., Cook, P. L. M., Wong, W. W., Hutchinson, T., Eate, V., et al. (2021). Hydrodynamic disturbance controls microbial community assembly and biogeochemical processes in coastal sediments. *The ISME Journal*, *16*(3), 750–763. https://doi.org/10.1038/s41396-021-01111-9

Chen, Y., Su, X., Wan, Y., Lyu, H., Dong, W., Shi, Y., & Zhang, Y. (2022). Nitrogen biogeochemical reactions during bank filtration constrained by hydrogeochemical and isotopic evidence: A case study in a riverbank filtration site along the second Songhua River, NE China. *Applied Geochemistry*, *140*, 105272. https://doi.org/10.1016/j.apgeochem.2022.105272

Clement, J., Pinay, G., & Marmonier, P. (2003). Seasonal dynamics of denitrification along topohydrosequences in three different riparian wetlands. *Journal of Environmental Quality*, *31*(3), 1025–1037. https://doi.org/10.2134/jeq2002.1025

DCNR. (2021). *Geology of Pennsylvania*. Pennsylvania Department of Conservation and Natural Resources (DCNR). Retrieved from https://www.dcnr.pa.gov/Geology/GeologyOfPA/Pages/default.aspx

Denk, T. R., Mohn, J., Decock, C., Lewicka-Szczebak, D., Harris, E., Butterbach-Bahl, K., et al. (2017). The nitrogen cycle: A review of isotope effects and isotope modeling approaches. *Soil Biology and Biochemistry*, *105*, 121–137. https://doi.org/10.1016/j.soilbio.2016.11.015

Dhondt, K., Boeckx, P., Van Cleemput, O., & Hofman, G. (2003). Quantifying nitrate retention processes in a riparian buffer zone using the natural abundance of ^{15}N in NO_3. *Rapid Communications in Mass Spectrometry*, *17*(23), 2597–2604. https://doi.org/10.1002/rcm.1226

Galloway, J. N., Townsend, A. R., Erisman, J. W., Bekunda, M., Cai, Z. C., Freney, J. R., et al. (2008). Transformation of the nitrogen cycle: Recent trends, questions, and potential solutions. *Science*, *320*(5878), 889–892. https://doi.org/10.1126/science.1136674

Giblin, A. E., Tobias, C. R., Song, B., Weston, N., Banta, G. T., & Rivera-Monroy, V. H. (2013). The importance of dissimilatory nitrate reduction to ammonium (DNRA) in the nitrogen cycle of coastal ecosystems. *Oceanography*, *26*(3), 124–131. https://doi.org/10.5670/oceanog.2013.54

Hansen, H. C. B., Koch, C. B., Nancke-Krogh, H., Borggaard, O. K., & Sørensen, J. (1996). Abiotic nitrate reduction to ammonium: Key role of green rust. *Environmental Science & Technology*, *30*(6), 2053–2056. https://doi.org/10.1021/es950844w

Herbert, E. R., Boon, P., Burgin, A. J., Neubauer, S. C., Franklin, R. B., Ardón, M., et al. (2015). A global perspective on wetland salinization: Ecological consequences of a growing threat to freshwater wetlands. *Ecosphere*, *6*(10), 1–43. https://doi.org/10.1890/es14-00534.1

Inamdar, S., Peipoch, M., Sena, M., Joshi, B., Rahman, M. M., Kan, J., et al. (2024). Riparian groundwater nitrogen (N) isotopes reveal human imprints of dams and road salt salinization [Dataset]. HydroShare. https://doi.org/10.4211/hs.5d326d1f18aa40738bf8bd7ec6e65eb9

Inamdar, S. P., Peck, E. K., Peipoch, M., Gold, A. J., Sherman, M., Hripto, J., et al. (2022). *Saturated, suffocated, and salty: Human legacies produce hot spots of nitrogen in riparian zones*. American Geophysical Union (AGU). https://doi.org/10.1029/2022jg007138

Jäntti, H., Aalto, S. L., & Paerl, H. W. (2021). Effects of ferrous iron and hydrogen sulfide on nitrate reduction in the sediments of an estuary experiencing hypoxia. *Estuaries and Coasts*, *44*(1), 1–12. https://doi.org/10.1007/s12237-020-00783-4

Kan, J., Peck, E. K., Zgleszewski, L., Peipoch, M., & Inamdar, S. (2023). Mill dams impact microbiome structure and depth distribution in riparian sediments. *Frontiers in Microbiology*, *14*, 1161043. https://doi.org/10.3389/fmicb.2023.1161043

Kendall, C., Elliott, E. M., & Wankel, S. D. (2007). Tracing anthropogenic inputs of nitrogen to ecosystems. In R. H. Michener, & K. Lajtha (Eds.), *Stable isotopes in ecology and environmental studies* (2nd ed., pp. 375–449). Wiley-Blackwell Publishing.

Lewis, E., Inamdar, S., Gold, A. J., Addy, K., Trammell, T. L. E., Merritts, D., et al. (2021). Draining the landscape: How do nitrogen concentrations in riparian groundwater and stream water change following milldam removal? *Journal of Geophysical Research: Biogeosciences*, *126*(8), e2021JG006444. https://doi.org/10.1029/2021jg006444

Lowrance, R., Altier, L. S., Newbold, J. D., Schnabel, R. R., Groffman, P. M., Denver, J. M., et al. (1997). Water quality functions of riparian forest buffers in Chesapeake Bay watersheds. *Environmental Management*, *21*(5), 687–712. https://doi.org/10.1007/s002679900060

Lutz, S. R., Trauth, N., Musolff, A., Van Breukelen, B. M., Knöller, K., & Fleckenstein, J. H. (2020). How important is denitrification in riparian zones? Combining end-member mixing and isotope modeling to quantify nitrate removal from riparian groundwater. *Water Resources Research*, *56*(1), e2019WR025528. https://doi.org/10.1029/2019wr025528

Matiatos, I., Wassenaar, L. I., Monteiro, L. R., Venkiteswaran, J. J., Gooddy, D. C., Boeckx, P., et al. (2021). Global patterns of nitrate isotope composition in rivers and adjacent aquifers reveal reactive nitrogen cascading. *Communications Earth & Environment*, *2*(1), 52. https://doi.org/10.1038/s43247-021-00121-x

Morina, J., & Franklin, R. (2022). Intensity and duration of exposure determine prokaryotic community response to salinization in freshwater wetland soils. *Geoderma*, *428*, 428. https://doi.org/10.1016/j.geoderma.2022.116138

Muggeo, V. M. (2008). Segmented: An R package to fit regression models with broken-line relationships. *R News*, *8*(1), 20–25.

Nestler, A., Berglund, M., Accoe, F., Duta, S., Xue, D., Boeckx, P., & Taylor, P. (2011). Isotopes for improved management of nitrate pollution in aqueous resources: Review of surface water field studies. *Environmental Science and Pollution Research International*, *18*(4), 519–533. https://doi.org/10.1007/s11356-010-0422-z

Neubauer, S. C., Piehler, M. F., Smyth, A. R., & Franklin, R. B. (2019). Saltwater intrusion modifies microbial community structure and decreases denitrification in tidal freshwater marshes. *Ecosystems*, *22*(4), 912–928. https://doi.org/10.1007/s10021-018-0312-7

Nikolenko, O., Jurado, A., Borges, A. V., Knller, K., & Brouyre, S. (2018). Isotopic composition of nitrogen species in groundwater under agricultural areas: A review. *Science of the Total Environment*, *621*, 1415–1432. https://doi.org/10.1016/j.scitotenv.2017.10.086

NOAA. (2021). State College, PA: National Weather Service Forecast Office. Retrieved from https://www.weather.gov/ctp/

Palacin-Lizarbe, C., Camarero, L., Hallin, S., Jones, C. M., Cáliz, J., Casamayor, E. O., & Catalan, J. (2019). The DNRA-denitrification dichotomy differentiates nitrogen transformation pathways in mountain lake benthic habitats. *Frontiers in Microbiology*, *10*, 1229. https://doi.org/10.3389/fmicb.2019.01229

Pan, W., Kan, J., Inamdar, S., Chen, C., & Sparks, D. (2016). Dissimilatory microbial iron reduction release DOC (dissolved organic carbon) from carbon-ferrihydrite association. *Soil Biology and Biochemistry*, *103*, 232–240. https://doi.org/10.1016/j.soilbio.2016.08.026

Pandey, C. B., Kumar, U., Kaviraj, M., Minick, K., Mishra, A., & Singh, J. (2020). DNRA: A short-circuit in biological N-cycling to conserve nitrogen in terrestrial ecosystems. *The Science of the Total Environment*, *738*, 139710. https://doi.org/10.1016/j.scitotenv.2020.139710

Peck, E., Inamdar, S., Sherman, M., Hripto, J., Peipoch, M., Gold, A., & Addy, K. (2022). Nitrogen sinks or sources? Denitrification and nitrogen removal potential in riparian legacy sediment terraces affected by milldams. *Journal of Geophysical Research: Biogeosciences*, *127*(10), e2022JG007004. https://doi.org/10.1029/2022JG007004

Peck, E. K., Inamdar, S. P., Peipoch, M., & Gold, A. J. (2023). Influence of relict milldams on riparian sediment biogeochemistry. *Journal of Soils and Sediments*, *23*(6), 2584–2599. https://doi.org/10.1007/s11368-023-03507-w

Peipoch, M., Martí, E., & Gacia, E. (2012). Variability in $\delta^{15}N$ natural abundance of basal resources in fluvial ecosystems: A meta-analysis. *Freshwater Science*, *31*(3), 1003–1015. https://doi.org/10.1899/11-157.1

Peralta, A., Ludmer, S., & Kent, A. (2013). Hydrologic history influences microbial community composition and nitrogen cycling under experimental drying/wetting treatments. *Soil Biology and Biochemistry*, *66*, 29–37. https://doi.org/10.1016/j.soilbio.2013.06.019

Pinay, G., Bernal, S., Abbott, B. W., Lupon, A., Marti, E., Sabater, F., & Krause, S. (2018). Riparian corridors: A new conceptual framework for assessing nitrogen buffering across biomes. *Frontiers in Environmental Science*, *6*(11). https://doi.org/10.3389/fenvs.2018.00047

Rahman, M. M., Roberts, K. L., Warry, F., Grace, M. R., & Cook, P. L. M. (2019). Factors controlling dissimilatory nitrate reduction processes in constructed stormwater urban wetlands. *Biogeochemistry*, *142*(3), 375–393. https://doi.org/10.1007/s10533-019-00541-0

Ramsey, K. W. (2005). *GM13 geologic map of new castle county, Delaware*. Delaware Geological Survey.

Ranalli, A. J., & Macalady, D. L. (2010). The importance of the riparian zone and in-stream processes in nitrate attenuation in undisturbed and agricultural watersheds—A review of the scientific literature. *Journal of Hydrology (Amsterdam)*, *389*(3), 406–415. https://doi.org/10.1016/j.jhydrol.2010.05.045

Reverey, F., Ganzert, L., Lischeid, G., Ulrich, A., Premke, K., & Grossart, H. P. (2018). Dry-wet cycles of kettle hole sediments leave a microbial and biogeochemical legacy. *The Science of the Total Environment*, *627*, 985–996. https://doi.org/10.1016/j.scitotenv.2018.01.220

Rivett, M. O., Buss, S. R., Morgan, P., Smith, J. W., & Bemment, C. D. (2008). Nitrate attenuation in groundwater: A review of biogeochemical controlling processes. *Water Research*, *42*(16), 4215–4232. https://doi.org/10.1016/j.watres.2008.07.020

Roberts, K., Grace, M., Cook, P., Erler, D., & Wong, W. W. (2023). Stable isotopes of nitrate ($\delta^{15}N$ and $\delta^{18}O$) as functional indicators of nitrogen processing in constructed wetlands. *Science of the Total Environment*, *899*, 165246. https://doi.org/10.1016/j.scitotenv.2023.165246

Robertson, E. K., Roberts, K. L., Burdorf, L. D. W., Cook, P., & Thamdrup, B. (2016). Dissimilatory nitrate reduction to ammonium coupled to Fe (II) oxidation in sediments of a periodically hypoxic estuary. *Limnology & Oceanography*, *61*(1), 365–381. https://doi.org/10.1002/lno.10220

Robertson, E. K., & Thamdrup, B. (2017). The fate of nitrogen is linked to iron(II) availability in a freshwater lake sediment. *Geochimica et Cosmochimica Acta*, *205*, 84–99. https://doi.org/10.1016/j.gca.2017.02.014

Rutting, T., Boeckx, P., Müller, C., & Klemedtsson, L. (2011). Assessment of the importance of dissimilatory nitrate reduction to ammonium for the terrestrial nitrogen cycle. *Biogeosciences*, *8*(7), 1779–1791. https://doi.org/10.5194/bg-8-1779-2011

Sebilo, M., Billen, G., Grably, M., & Mariotti, A. (2003). Isotopic composition of nitrate-nitrogen as a marker of riparian and benthic denitrification at the scale of the whole seine river system. *Biogeochemistry*, *63*(1), 35–51. https://doi.org/10.1023/A:1023362923881

Sherman, M., Hripto, J., Peck, E., Gold, A., Peipoch, M., Imhoff, P., & Inamdar, S. (2022). Backed-up, saturated, and stagnant: Effect of milldams on upstream riparian groundwater hydrologic and mixing regimes. *Water Resources Research*, *58*(10), e2022WR033038. https://doi.org/10.1029/2022WR033038

Shi, W., Chen, Q., Zhang, J., Zheng, F., Liu, D., Yi, Q., & Chen, Y. (2020). Enhanced riparian denitrification in reservoirs following hydropower production. *Journal of Hydrology (Amsterdam)*, *583*, 124305. https://doi.org/10.1016/j.jhydrol.2019.124305

Straub, K. L., Benz, M., Schink, B., & Widdel, F. (1996). Anaerobic, nitrate-dependent microbial oxidation of ferrous iron. *Applied and Environmental Microbiology*, *62*(4), 1458–1460. https://doi.org/10.1128/aem.62.4.1458-1460.1996

Tiedje, J. M. (1988). Ecology of denitrification and dissimilatory nitrate reduction to ammonium. In A. B. J. Zehnder (Ed.), *Environmental microbiology of anaerobes* (pp. 179–244). John Wiley & Sons.

Tomasek, A. A., Hondzo, M., Kozarek, J. L., Staley, C., Wang, P., Lurndahl, N., & Sadowsky, M. J. (2019). Intermittent flooding of organic-rich soil promotes the formation of denitrification hot moments and hot spots. *Ecosphere*, *10*(1). https://doi.org/10.1002/ecs2.2549

Vidon, P., & Hill, A. R. (2005). Denitrification and patterns of electron donors and acceptors in eight riparian zones with contrasting hydrogeology. *Biogeochemistry*, *71*(2), 259–283. https://doi.org/10.1007/s10533-005-0684-6

Wang, R., Xub, S., Zhang, M., Ghulam, A., Dai, C., & Ping Zheng, P. (2020). Iron as electron donor for denitrification: The efficiency, toxicity and mechanism. *Ecotoxicology and Environmental Safety*, *194*, 110343. https://doi.org/10.1016/j.ecoenv.2020.110343

Wang, X., Wells, N. S., Xiao, W., Hamilton, J. L., Jones, A. M., & Collins, R. N. (2023). Abiotic reduction of nitrate to ammonium by iron (oxy)(hydr)oxides and its stable isotope ($\delta^{15}N$, $\delta^{18}O$) dynamics. *Geochimica et Cosmochimica Acta*, *347*, 28–41. https://doi.org/10.1016/j.gca.2023.02.013

Weber, K. A., Urrutia, M. M., Churchill, P. F., Kukkadapu, R. K., & Roden, E. E. (2006). Anaerobic redox cycling of iron by freshwater sediment microorganisms. *Environmental Microbiology*, *8*(1), 100–113. https://doi.org/10.1111/j.1462-2920.2005.00873.x

Weitzman, J. N., Brooks, J. R., Mayer, P. M., Rugh, W. D., & Compton, J. E. (2021). Coupling the dual isotopes of water (δ^2H and δ^{18}O) and nitrate (δ^{15}N and δ^{18}O): A new framework for classifying current and legacy groundwater pollution. *Environmental Research Letters*, *16*(4), 1–45008. https://doi.org/10.1088/1748-9326/abdcef

Weston, N. B., Giblin, A. E., Banta, G. T., Hopkinson, C. S., & Tucker, J. (2010). The effects of varying salinity on ammonium exchange in estuarine sediments of the parker river, Massachusetts. *Estuaries and Coasts*, *33*(4), 985–1003. https://doi.org/10.1007/s12237-010-9282-5

Ye, C., Cheng, X., Zhang, K., Du, M., & Zhang, Q. (2017). Hydrologic pulsing affects denitrification rates and denitrifier communities in a revegetated riparian ecotone. *Soil Biology and Biochemistry*, *115*, 137–147. https://doi.org/10.1016/j.soilbio.2017.08.018

Zhu, Y., Dai, H., & Yuan, S. (2023). The competition between heterotrophic denitrification and DNRA pathways in hyporheic zone and its impact on the fate of nitrate. *Journal of Hydrology*, *626*, 130175. https://doi.org/10.1016/j.jhydrol.2023.130175